International Journal of Refractory Metals & Hard Materials 72 (2018) 97–103

Contents lists available at ScienceDirect

International Journal of Refractory Metals & Hard Materials

journal homepage: www.elsevier.com/locate/IJRMHM

Recrystallization and composition dependent thermal fatigue response of different tungsten grades

G. Pintsuk[a,*], S. Antusch[b], T. Weingaertner[b], M. Wirtz[a]

[a] Forschungszentrum Jülich GmbH, Institute for Energy and Climate Research, Partner of the Trilateral Euregio Cluster (TEC), 52425 Jülich, Germany
[b] Karlsruhe Institute of Technology (KIT), Institute for Applied Materials, 76344 Eggenstein-Leopoldshafen, Germany

ARTICLE INFO

Keywords:
Tungsten
Recrystallization
Thermal fatigue
High heat flux

ABSTRACT

Industrial pure tungsten grades, manufactured by using a variety of manufactured techniques, are available worldwide in many different types of semifinished products, i.e. rods, wires, ribbons, and sheets. Thereby, the recrystallization temperature varies depending on the applied degree of deformation but also depending on the materials composition, i.e. the materials purity and in particular the level of certain impurities.

In order to compare different available industrial tungsten grades and a newly developed PIM-W grade, on the one hand recrystallization studies at three different temperatures from 1573 to 2073 K for 1 h were performed using microstructural analyses and Vickers hardness testing. On the other hand, the thermal shock induced low cycle thermal fatigue response of the material in its different recrystallization stages was done using high heat flux tests at 1273 K base temperature, applying 1000 shots with 1 ms and 0.38 GW/m^2 and post-mortem characterization, i.e. profilometry and metallography. The obtained results are related to the microstructural and mechanical features of the materials as well as the chemical composition of the individual tungsten grades.

1. Introduction

The use of tungsten as plasma facing material for future nuclear fusion applications is on the one hand related to its beneficial properties like high melting temperature, good thermal conductivity and low tritium inventory. On the other hand, its brittleness at low temperatures and its recrystallization and therefore softening at high temperatures puts high demands on the component design as well influences the allowed operational temperature limits. Besides, also the material itself, its related manufacturing technology and impurity concentration, is expected to play a decisive role as it influences the materials microstructure, its anisotropic material properties and also recrystallization.

For the next step fusion device ITER ("The Way" in Latin) actually being built in Cadarache, France, tungsten monoblock-shaped components and qualification mock-ups schematically shown in Fig. 1 have been produced in Europe and Japan for the use in the divertor of the device [1,2,3,4]. These mock-ups not only use different tungsten grades from European and Russian on the one hand and Japanese manufacturers on the other hand but are also produced using different manufacturing technologies, i.e. hot isostatic pressing (HIP) and hot radial pressing (HRP) in Europe and brazing in Japan. Thereby, the manufacturing technology has to guarantee a sufficient remaining strength of the CuCrZr-tube acting as structural material, which requires dedicated annealing and temperating treatments depending on the process temperature during joining.

The manufactured mock-ups have been tested in electron beam facilities in France and Russia up to 1000 cycles at 20 MW/m^2 with 10 s loading and 10 s dwell time showing a different surface response depending on the used electron beam (beam diameter: locally induced thermal shock loads during beam scanning) and also a varying response with respect to the formation of macro-cracks (Fig. 1) for European and Japanese manufacturers [4,3,5]. While macro-cracks were found for all European manufacturers and an increased number of cracks was found in case of the existence of electron beam induced surface cracking acting as potential crack initiation points (modelling by Li et al. [6]), no macro-crack formation was found for the Japanese mock-ups. The influencing factors are assumed to be the thermal and mechanical resistance of the individual tungsten grades and the manufacturing technology. However, also the design of the components and in particular the geometrical dimensions of the tungsten block seem to play a decisive role, e.g. no crack formation was found for previously investigated designs with 23 mm block width and 10 mm inner cooling tube diameter, while crack formation occurs frequently in case of the actual design with 28 mm width. This observation is in agreement with the findings from modelling studies on the influence of the component size [7].

* Corresponding author.
E-mail address: g.pintsuk@fz-juelich.de (G. Pintsuk).

https://doi.org/10.1016/j.ijrmhm.2017.11.039
Received 21 September 2017; Accepted 25 November 2017
Available online 14 December 2017

Fig. 1. a) Schematic view of a tungsten monoblock mock-up consisting of a CuCrZr-tube with 12 mm inner diameter and a thickness of 1.5 mm, a 1 mm pure copper interlayer and surrounding tungsten blocks with 28 × 12 mm front surface and a varying height (plasma front thickness 5.5 to 8 mm); b) Top view of such a mock-up with 7 tungsten blocks after testing at 20 MW/m^2.

In any case, by comparison of the results from the two different electron beam facilities, the statistical appearance of macro-cracks is significantly increased as soon as shallow surface cracks, introduced by the electron beam, are present. As such shallow cracks may also appear during operation as a result of highly frequent Edge Localized Modes (ELMs) applying thermal shock loads in the range of up to the GW/m^2 range in non-mitigated condition for about 0.5 ms.

The investigations herein focus on the characterization of the different commercially available tungsten grades that have been used for the fabrication of the European and Japanese mock-ups in comparison with a tungsten grade manufactured via powder injection molding (PIM) providing an isotropic and recrystallized microstructure directly after the manufacturing process. Thereby, the thermal shock induced thermal fatigue performance of the materials is determined in dependence on the materials microstructure, not only with respect to the manufacturing technology but also to their recrystallization behavior. These investigations should provide an answer to the question on the influence of the material on the formation of macro-cracks in the actively cooled components and provide information about damage characteristics due to thermal shock loading that have to be taken into account for the component design.

2. Materials microstructural and mechanical characterization

2.1. Tungsten grades & recrystallization

In the frame of this work, four different tungsten products were investigated, i.e. powder injection molded pure W produced by KIT (PIM-W) [8–10], a forged bar material produced by PLANSEE AG (W-PL), and rolled plate materials from POLEMA JSC (W-PO) and A.L.M.T. Corp (W-AL).

The industrially produced bar and plate materials, all of them fulfilling the actual specifications for the use as plasma facing material in ITER and being used for the manufacturing of the before mentioned ITER mock-ups, are characterized by an anisotropic grain structure and related material properties due to the applied deformation processes for densification. In contrast, PIM-W, being produced not yet at the industrial but medium scale level, exhibits a fully isotropic grain structure in the recrystallized state due to high final sintering temperatures > 2473 K (Fig. 2, left column).

The materials were characterized by chemical analyses to determine the exact composition of the investigated batch and any potential influence that may contribute to observed differences in the material behavior. The analyses were done by ICP-OES and ICP-MS for most of the elements while ON were analyzed by hot gas extraction and CS with a CS-analyzer. The obtained results are provided in Table I and indicate that O, Cr, Fe, Ni, Cu and Mo are the main impurities still on a low ppm level. Thereby, W-AL exhibits the highest purity among all investigated materials.

From the materials, small thermo-shock specimens with the size of 10 × 10 × 4 mm were cut by EDM in such a way, that the deformation direction of the grains is perpendicular to the surface. This orientation represents the configuration, which will be finally used for the manufacturing of actively cooled plasma facing components. Subsequently, individual specimens were annealed in a tungsten vacuum furnace (10^{-4}–10^{-5} mbar) at 1573 K, 1773 K and 2073 K for 1 h in Al_2O_3 crucibles. The heating rate was 10 K/min and the cooling rate for 1573 K and 1773 K was 10 K/min for 20 min followed by adiabatic cooling. For annealing at 2073 K, in order to protect the furnace and the used crucibles, the cooling rate was 6.7 K/min till 1873 K, 10 K/min till 1673 K, 12 K/min till 1373 K and finally adiabatic cooling. This aims for the determination of the onset of recrystallization for the particular material and the influence of recrystallization on the mechanical and in particular thermal-shock induced thermal fatigue performance of the material. After recrystallization both the reference and the annealed specimens were polished on one front surface to a mirror finish with a roughness R_a of ~0.1 μm.

In Fig. 2 the different microstructures of the materials as a function of the annealing treatment are shown with the view on the surface plane that will be exposed to the high heat flux loads. As mentioned before, the grain size (Fig. 3) and shape varies strongly between the different materials in their reference state. Thereby, for PIM-W it has to be taken into account that due to the net-shape production method without any further post-treatment it is characterized by a dual microstructure (Fig. 4a). This microstructure consists of a surface near seam of about 0.5 mm thickness exhibiting grains with a size of up to several hundred micrometers (surface near, i.e. the first 100–150 μm the grain size is smaller as shown in Fig. 4b) and a bulk grain structure with an average grain diameter of ~40 μm. As the thermal shock testing is a surface-near process, the material characteristics provided in the following are limited to those representing the surface-near region.

While PIM-W shows large isotropic grains whose shape and average size does not vary as a function of the annealing temperature, W-PL is characterized in the reference state by significantly smaller grains with a needle like structure oriented perpendicular to the surface. Due to annealing the anisotropy of the grains vanishes, partially at 1573 K and fully at 1773 K, and the size of the recrystallized grains is about 30% larger than the one for PIM-W. W-PO and W-AL, both rolled materials with a plate like grain structure with one deformation direction in the surface plane and the other perpendicular to the surface, exhibit a significantly smaller grain size with an elongation ratio of 1:4 and while here the recrystallization seems to be finalized already after annealing at 1573 K (almost in case of W-AL), the grain sizes are about 50% below those for PIM-W.

In addition, Auger electron spectroscopy of the fracture surfaces of the different materials were performed to determine existing impurities within the grains and at the grain boundaries. It was shown that the investigated specimens from W-PO and W-AL, in contrast to W-PL (for PIM-W the results were not conclusive), exhibit a small amount of phosphorus at the intergranular surfaces. In all cases, no phosphorus was found on the cleavage planes. How these findings correlate with the recrystallization performance of the material will be discussed below.

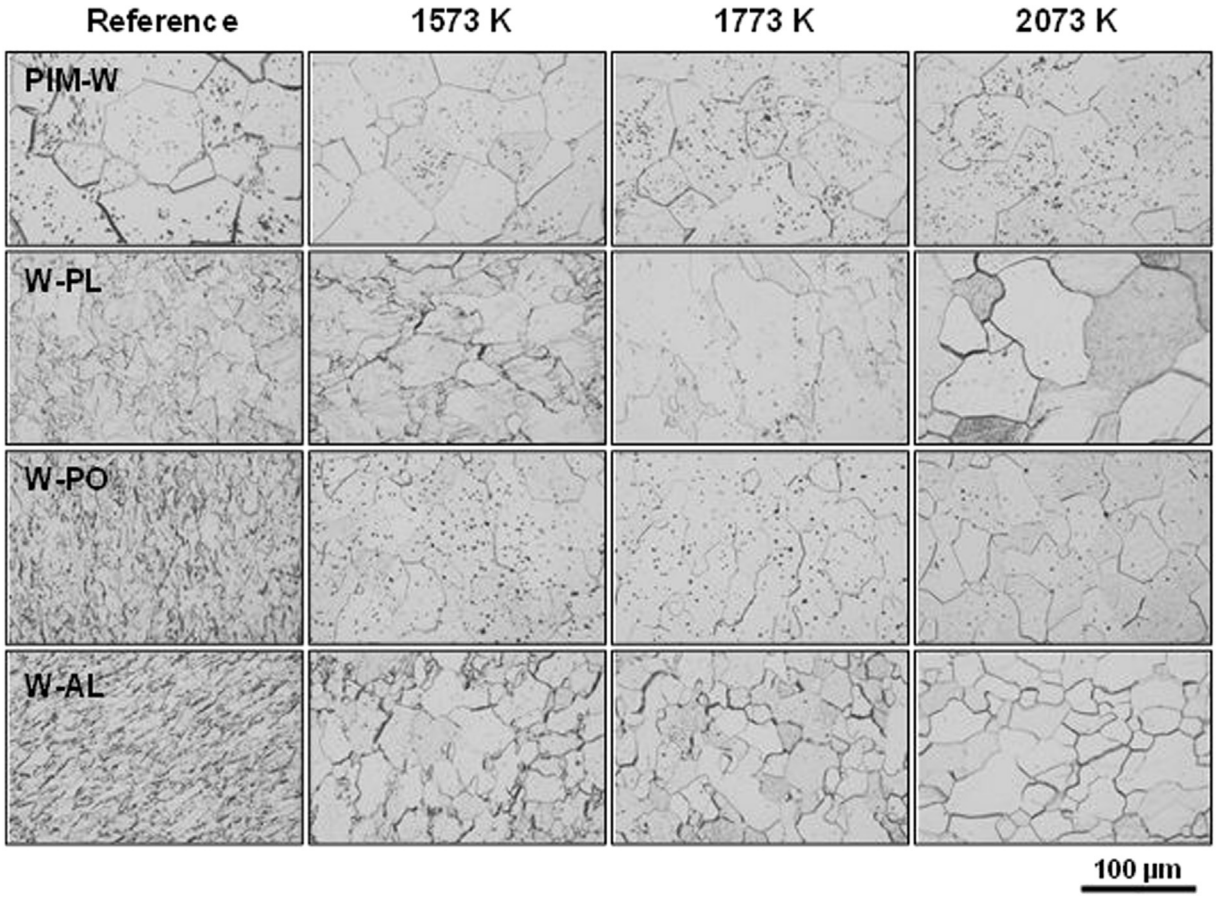

Fig. 2. Light microscopy images of the grain structure of the tungsten grades in the reference state and after annealing – view on the surface that is also exposed to the high heat flux loads.

Table I
Chemical analyses of the four different investigated tungsten products.

Element	Unit	PIM-W	W-PL	W-PO	W-AL
C	ppm	671 ± 125	< 4	< 4	< 4
N	ppm	< 2	< 2	< 2	< 2
O	ppm	< 2	13 ± 5	10	8 ± 7
Al	ppm	< 2	< 3	< 3	< 3
S	ppm	< 4	< 4	< 4	< 4
K	ppm	< 5	< 1	< 1	< 1
Cr	ppm	4.2 ± 0.1	1.1 ± 0.1	1.2 ± 0.04	< 0.3
Fe	ppm	29 ± 2	5.2 ± 0.7	9.5 ± 0.4	1.4 ± 0.3
Ni	ppm	1.7 ± 0.1	< 0.4	5.1 ± 0.04	< 0.4
Cu	ppm	0.7 ± 0.07	3.4 ± 1.5	1.2 ± 0.4	0.4 ± 0.1
Mo	ppm	< 0.1	5.1 ± 0.6	14.3 ± 0.7	< 0.7
Ta	ppm	< 0.2	< 0.2	0.5 ± 0.02	< 0.2
Re	ppm	< 2	< 2	< 2	< 2

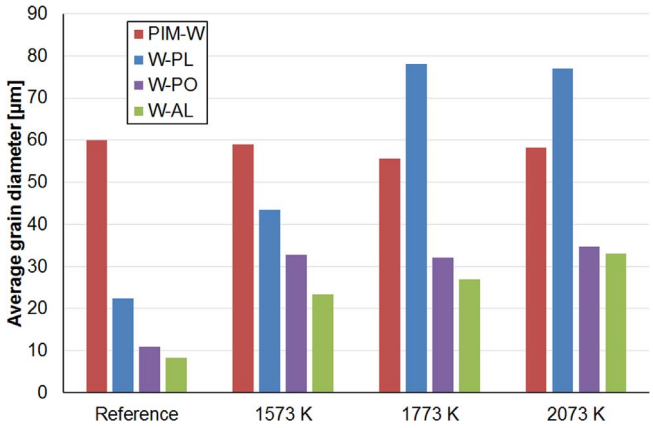

Fig. 3. Average grain size of all investigated materials measured at the top surface as a function of the annealing temperature; for W-PO and W-AL in the reference state the value represents the size perpendicular to the elongation orientation with an elongation ratio of 1:4.

2.1.1. Mechanical investigation

Vickers hardness HV2 was measured at the polished and high heat flux exposed surface of the thermal shock specimens and the results are illustrated in Fig. 5. While the industrially produced W-products in their reference state exhibit a hardness of 430–460 HV2, PIM-W is characterized by a medium hardness of ~350–360 HV2, a typical value for recrystallized tungsten, resulting from the production process. Accordingly, there is no impact of annealing treatment on the hardness and mechanical properties of PIM-W and the observed minor variations are within the measurement error.

For all the industrial W-products, reduction of hardness and therefore recrystallization takes place starting from 1573 K at different velocities for the three materials. According to the actual results, W-PO and W-AL are fully recrystallized after the applied annealing treatment even at the lowest temperature with hardness values of 350–370 HV2, which confirms the finding of the microstructural observation. In contrast, for W-PL the recrystallization process has started but not finished after annealing at 1573 K with a still remaining hardness > 400 HV2. These results are surprising, in particular in view of previous investigations on the same materials grades (except W-PO from different batches; annealing performed in the same furnace using identical conditions) but using HV30 instead of HV2 [11]. Thereby, neither W-PO nor W-AL showed recrystallization after annealing at 1573 K while W-PL was fully recrystallized at the same temperature. Even more, W-AL still provided a hardness of ~420 HV30 even after annealing at 1773 K.

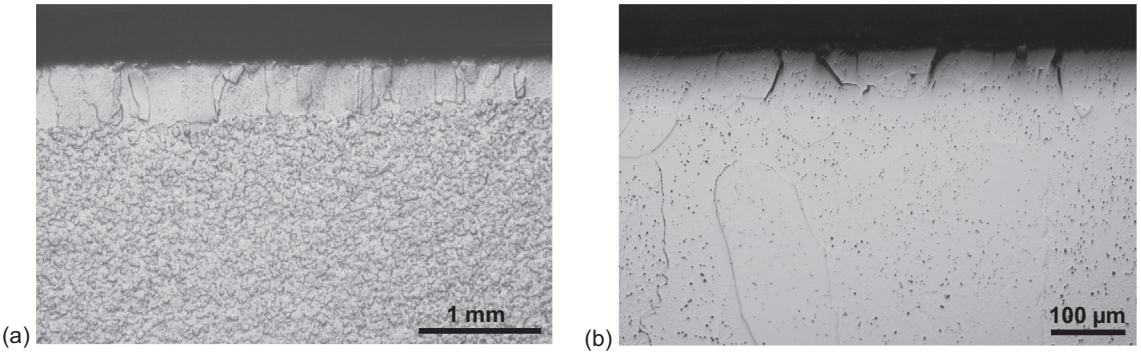

Fig. 4. Cross section of PIM-W showing a dual microstructure due to final shape sintering without post-sintering treatment; a) overview and b) surface near view after annealing at 2073 K and thermal shock loading.

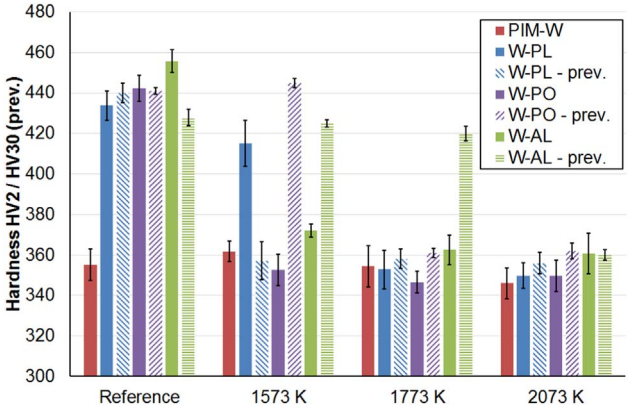

Fig. 5. Vickers hardness of the individual tungsten products measured before and after the annealing treatment with data included from [11].

In order to exclude an influence of the measurement load and therefore the tested material area and volume of the hardness test, the hardness of the herein investigated W-AL after annealing at 1773 K was determined to be 375 ± 4 HV30, which is in fair agreement with the HV2 value (362.5 ± 7.4).

An explanation for the higher recrystallization resistance in previous analyses of those materials would have been the existence of phosphorus at the grain boundaries. However, the strong discrepancy to the actual results with an improvement for W-PL and a reduction of performance for W-PO and W-AL, even if in case of W-PO the identical material batch was investigated, raises several questions with regard to the reproducibility of material batches and the homogeneity within individual batches.

Related mechanical data for the industrially produced materials obtained by tensile testing at 1073 K can be found in [M. Wirtz (IAEA, NF)]. Thereby, W-PO shows in the reference state always the highest yield and tensile strength as well as total elongation, while the performance after annealing at 2073 K is identical among all materials within the measurement error.

2.2. High heat flux testing and post-mortem characterization

High heat flux testing was performed in the electron beam facility JUDITH 1 at Forschungszentrum Jülich, being characterized by a beam diameter of ~1 mm at full width half and a triangular scanning mode in the x- and y-direction with kHz frequency. For the tests, specimens from the materials with anisotropic grain structure were prepared in such a way that the direction of the grain elongation is perpendicular to the heat loaded surface. The size of the loaded specimens was 10 × 10 × 4 mm while the loaded area of 4 × 4 mm^2 was located in the center of the front surface, which was polished to an arithmetic mean surface roughness R_a of 0.1 µm. For obtaining a flat profile a set frequency of ~41 and 30 kHz in x- and y-direction was used, respectively. The tests were performed by applying 1000 thermal shock loads with a pulse duration of 1 ms at a base temperature of 1273 K with a power density of 0.38 GW/m^2. These conditions were chosen as they are in the same range as edge localized modes (ELMs), i.e. frequent loads (> 1 Hz) that are expected to occur in a nuclear fusion device during normal operation. Furthermore, they are above the damage threshold for tungsten allowing a comparison of the different materials and annealing states based on the occurring damage.

The temperature increase during such a transient event can be calculated by using the equation provided in [12]. Using 114 W/m·K, 152 J/kg·K and 19,260 kg/m^3 as material input parameters at 1273 K, the surface temperature increase during the thermal shock pulse is expected to be ~740 K and accordingly the surface temperature will achieve ~2000 K corresponding roughly to the maximum temperature used for the annealing treatment. Assuming homogeneous loading and using an expansion coefficient of ~4.9 × 10^{-6} K^{-1} at 1273 K for tungsten the thermal expansion and the deformation rate of the 4 × 4 mm^2 area during the thermal shock heating amounts to ~15 µm and ~15 mm/s, respectively. This thermal induced expansion leads to compressive forces on the loaded area, which is surrounded and therefore constrained by “cold” material, and accordingly a compression by ~15 µm or 0.375%, which is in the plastic deformation regime. This regime was chosen to definitely obtain evaluable thermal fatigue induced material damage when applying the 1000 pulses that can be achieved within a reasonable time in the used device and which represents a standard testing procedure for the qualification of newly developed tungsten grades and tungsten composites. More detailed investigations on thermal fatigue and in particular damage thresholds at significantly lower loads (about a factor 4) and higher pulse numbers in the range of 10^6 to 10^7 can only be performed in the electron beam facility JUDITH 2, but are significantly more time consuming and therefore are done only for selected materials [13].

The damage evaluation was performed in post-mortem analyses by (1) profilometry for the determination of the arithmetic mean surface roughness R_a, (2) scanning electron microscopy for the determination of crack formation and appearance and (3) metallography for the determination of crack path and length. By correlation of the profilometric results shown in Fig. 6 with the microstructural observation and the hardness measurements, the first observation is that as expected PIM-W provides a stable behavior in any condition. However, due to its lowest hardness and largest grain size it provides the lowest performance in its reference state with an about a factor 2 higher roughness compared with the other industrially manufactured materials, which are about at the same level with slight advantages for W-PO. The second finding is that after annealing at 1573 K the roughness for all industrial grades increase, providing in particular for W-PO and W-AL comparably high roughness values even beyond those for PIM-W. The reason for this

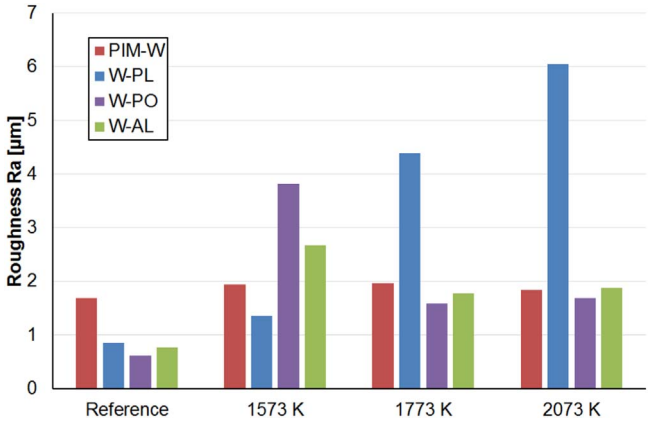

Fig. 6. Arithmetic mean surface roughness R_a of the loaded areas of the individual tungsten products.

might be the still ongoing recrystallization process with an already reduced mechanical strength and pre-existing material inhomogeneities in the industrially produced materials.

The occurrence of inhomogeneities is confirmed by the appearance of the loaded area showing islands of large crack formation as shown in Fig. 7a for W-AL. These inhomogeneities are found for W-PO and W-AL already in the reference state and still exist and show a strongly pronounced crack formation after annealing at 1573 K while at higher annealing temperatures and accordingly for a fully recrystallized microstructure they almost vanish (Fig. 7b) leading to roughness values comparable with PIM-W. In contrast, for W-PL the number of inhomogeneities and the damage occurring in these regions continuously increases (Fig. 8) leading to a significant surface roughening that exceeds those of the other materials after annealing at 2073 K by a factor 3. This is in contrast to the microstructural observations and hardness results where saturation starts at an annealing temperature of 1773 K and accordingly a further material degradation was not expected.

Besides these inhomogeneities, the appearance of cracks is identical for all materials in their recrystallized states and representatively shown for PIM-W in Fig. 9. Thereby, crack distances are in the range of single grains with some grains still partially being attached to each other. However, the surface shows “cluster” formaton of several grains surrounded by large cracks with a width of several tens micrometer while within the cluster the crack width varies from almost closed to a few micrometer. This distribution is owed to the fact that thermal fatigue induced crack formation occurs consecutively starting with the stress relieving cracks around the grain clusters followed by further crack formation within the clusters as a function of the number of pulses.

For the materials in their reference state, the crack distance is in general similar to those of the recrystallized materials and representatively shown for W-AL in Fig. 10. The maximum found crack width is in the range of about 10 µm, which is significantly lower than for the recrystallized materials and owed to the higher mechanical strength. However, none of the materials was fully resistant to crack formation at these loading conditions.

The investigation of the cross section showed that, independent of the material, the maximum crack depth varies in a narrow range between 40 and 60 µm. The crack path thereby runs along the grain boundaries and larger cracks, e.g. as shown in Fig. 9b, are correlated with an increased “delamination” of single grains (cf. Fig. 4b) that may in the long run, i.e. a higher number of pulses, lead to local overheating and possibly melting of single grains as has been shown in literature [13].

3. Conclusion

Based on the investigations on three different industrially produced tungsten grades being potential candidates for the use in ITER and a still developmental PIM-W grade produced by KIT, Germany, the findings are summarized below:

a) In the reference state, the industrially produced materials provide a higher thermal shock/thermal fatigue resistance compared to PIM-W and a comparable performance among each other.
b) There is no difference observable between rolled tungsten materials with respect to microstructure, recrystallization, hardness and thermal shock/thermal fatigue behavior.
c) After recrystallization rolled tungsten and PIM-W show an equivalent thermal shock/thermal fatigue behavior despite the factor 2 lower grain size for rolled materials.
d) After recrystallization forged tungsten shows larger grain sizes and further degradation with respect to the thermal shock/thermal fatigue behavior.
e) The chemical composition of the tungsten materials seems to play no major role.
f) The industrially produced materials show microstructural inhomogeneities in the reference state that are characterized by different damage formation, i.e. localized strong and large crack formation. After full recrystallization, these inhomogeneities vanish almost completely for the rolled materials while for the forged materials the amount and degradation by the inhomogeneities still increases, even when the recrystallization induced grain size increase saturates.
g) In comparison with earlier studies, the industrial materials coming from the same and also different batches exhibit strong variations in particular with regard to their recrystallization resistance.

From these finding, the following conclusions can be drawn:

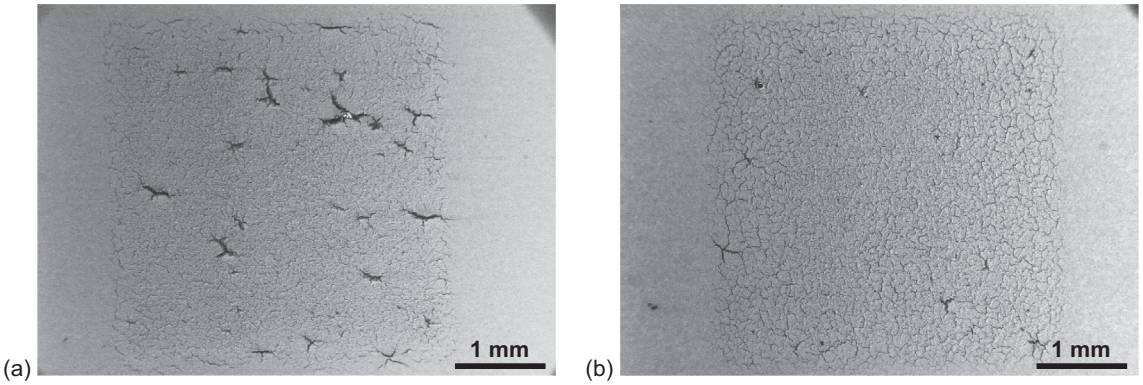

Fig. 7. Thermal shock loaded area (P = 0.38 GW/m^2, t = 1 ms, T_{base} = 1000 °C, n = 1000) of W-AL after annealing at a) 1573 K and b) 2073 K.

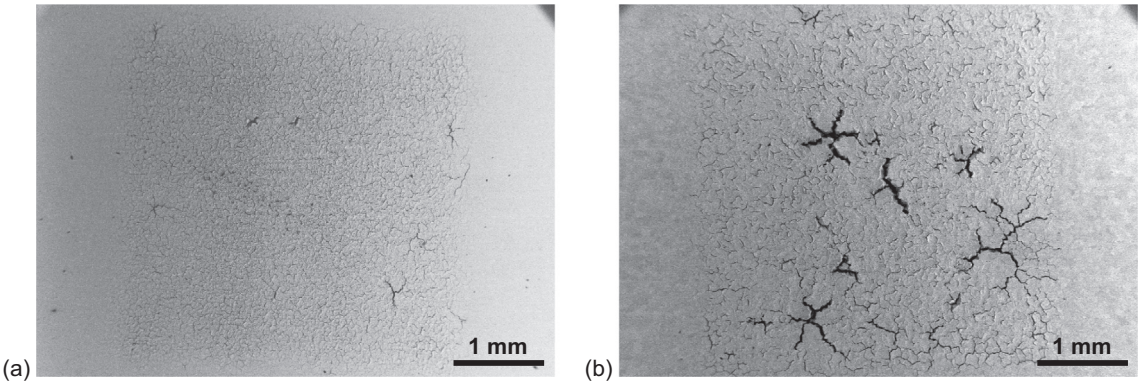

Fig. 8. Thermal shock loaded area (P = 0.38 GW/m^2, t = 1 ms, T_{base} = 1000 °C, n = 1000) of W-PL after annealing at a) 1573 K and b) 2073 K.

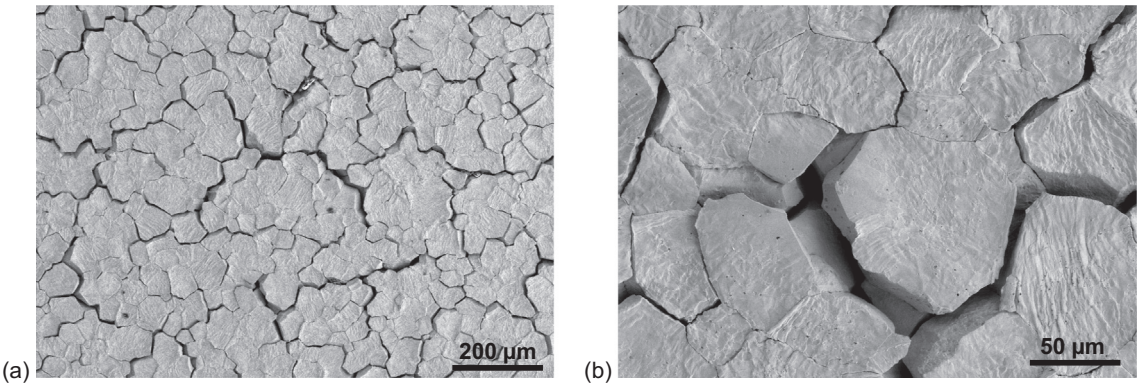

Fig. 9. Thermal shock loaded area (P = 0.38 GW/m^2, t = 1 ms, T_{base} = 1000 °C, n = 1000) of PIM-W after annealing at 2073 K with different magnification.

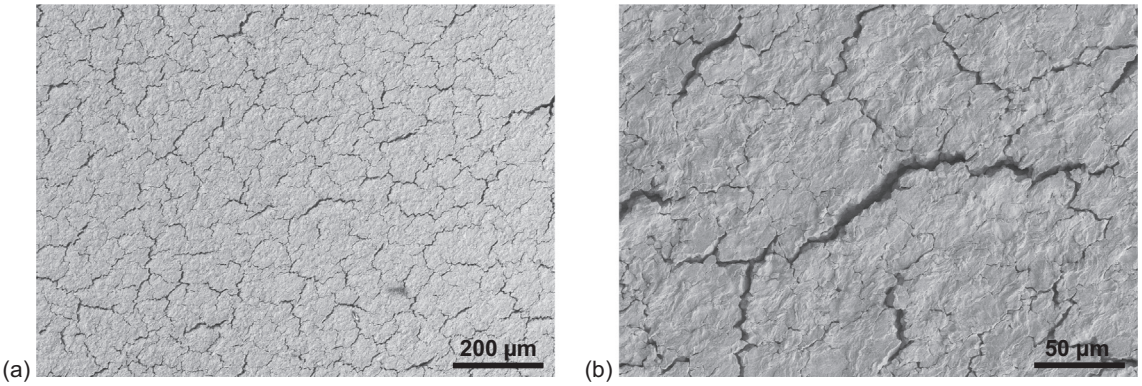

Fig. 10. Thermal shock loaded area (P = 0.38 GW/m^2, t = 1 ms, T_{base} = 1000 °C, n = 1000) of W-AL in the reference state.

(i) During the operation of ITER thermal shock/thermal fatigue induced crack formation using these tungsten grades is inevitable as long as the operational loads during ELMs are not significantly reduced and accordingly component design has to take these small and potential macro-crack initiation points into account.

(ii) As long as recrystallization of surface near parts of the component cannot be avoided during operation, PIM-W with respect to the short thermal transient and particle induced plasma wall interaction is an alternative option. The material's performance in those areas experiencing temperatures below the recrystallization threshold has to be qualified by separate design studies.

(iii) Due to the comparably small differences between the materials, the influence of the material on the macro-crack formation is expected to be low. However, the found variations within batches and between different batches requires further material qualification.

References

[1] M. Merola, F. Escourbiac, R. Raffray, P. Chappuis, T. Hirai, A. Martin, Fus. Eng. Des. 89 (2014) 890–895.
[2] K. Ezato, S. Suzuki, H. Yamada, T. Hirayama, K. Yokoyama, F. Escourbiac, T. Hirai, Fus. Eng. Des. 109–111 [Part B] (2016) 1256–1260.
[3] T. Hirai, F. Escourbiac, V. Barabash, A. Durocher, A. Fedosov, L. Ferrand, T. Jokinen, V. Komarov, M. Merola, S. Carpentier-Chouchana, N. Arkhipov, V. Kuznetcov, A. Volodin, S. Suzuki, K. Ezato, Y. Seki, B. Riccardi, M. Bednarek, P. Gavila, J. Nucl. Mater. 463 (2015) 1248–1251.
[4] P. Gavila, B. Riccardi, G. Pintsuk, G. Ritz, V. Kuznetsov, A. Durocher, Fus. Eng. Des. 98–99 (2015) 1305–1309.
[5] G. Pintsuk, M. Bednarek, P. Gavila, S. Gerzoskovitz, J. Linke, P. Lorenzetto, B. Riccardi, F. Escourbiac, Fus. Eng. Des. 98–99 (2015) 1384–1388.
[6] M. Li, J.-H. You, Fus. Eng. Des. 101 (2015) 1–8.
[7] M. Li, J.-H. You, Fus. Eng. Des. 113 (2016) 162–170.
[8] S. Antusch, D.E.J. Armstrong, T.B. Britton, L. Commin, J.S.K.-L. Gibson, H. Greuner, J. Hoffmann, W. Knabl, G. Pintsuk, M. Rieth, S.G. Roberts, T. Weingaertner, Nucl. Mat. Energy 3–4 (2015) 22–31.
[9] S. Antusch, J. Reiser, J. Hoffmann, A. Onea, Refract. Mater. Energy Appl. 7 (2017)

1064–1070, http://dx.doi.org/10.1002/ente.201600571.
[10] S. Antusch, L. Commin, M. Mueller, V. Piotter, T. Weingaertner, J. Nucl. Mater. 447 (2014) 314–317.
[11] M. Wirtz, I. Uytdenhouwen, V. Barabash, F. Escourbiac, T. Hirai, J. Linke, Th. Loewenhoff, S. Panayotis, G. Pintsuk, Nucl. Fusion 57 (2017) 066018.
[12] T. Hirai, G. Pintsuk, Fus. Eng. Des. 82 (2007) 389–393.
[13] M. Wirtz, J. Linke, Th. Loewenhoff, G. Pintsuk, I. Uytdenhouwen, Nucl. Mat. Energy 12 (2017) 148–155.